Original Article

Alexander Scharf*, Benedikt Neyses and Dick Sandberg

Hardness of surface-densified wood. Part 2: prediction of the density profile by hardness measurements

https://doi.org/10.1515/hf-2021-0232
Received November 26, 2021; accepted January 26, 2022;
published online March 8, 2022

Abstract: The density profile of surface-densified wood has a major influence on the indentation resistance of the material. A method that can predict the density profile in surface-densified wood from measurements of the indentation in a hardness test was established. The combined information of hardness and density profile is expected to better assess the performance of surface-densified wood. Density profile and hardness test data for surface-densified Scots pine have been subjected to a partial least squares analysis to determine the relationship between the indentation depth measured during a hardness test and the density profile measured by X-ray densitometry. Among seven different hardness tests, which varied in test force and indenter geometry, the Brinell method according to the EN 1534 standard showed the highest correlation between the indentation-versus-time curve and the density profile. The mean absolute error for the prediction of density profiles in an external test set was 5–10%, indicating that the method proposed in this study can be used to replace X-ray densitometry in process control and process design.

Keywords: densification; partial least squares regression; wood compression.

1 Introduction

Surface densification of wood increases the hardness and wear resistance of the surface for use in products such as flooring and table tops, where the surface is of primary interest. Through thermomechanical compression, it is possible to steer the degree of compression of the wood cells immediately beneath the surface and also the shape and location of the "peak region" of the through-thickness density profile (DP) as it was shown for particle boards (Hänsel et al. 1988). The DP has a large influence on the measured hardness (Laine et al. 2013). Part 1 of this study (Scharf et al. 2022) showed that even though hardness is a commonly measured property of surface-densified wood, it should not be used as a material property, as the obtained hardness values are strongly dependent on test parameters and test material homogeneity (Rautkari et al. 2011). It is proposed that the DP itself can be used as the true indicator of the material properties.

A hardness number acquired according to standardised test methods represents only the final moments of the hardness test, neglecting the previous response of the material to the test load. Two specimens, exhibiting the same hardness, may show a different indentation-versus-time curve, yet exhibit the same hardness value (Figure 1).

Part 1 of this study and Neyses et al. (2017) found that the slope of the indentation versus-time curve in an indentation test is dependent on the DP in the hardness test direction and consequently embeds information of the surface properties. This indicates that the continuous measurement of indentation depth during a hardness test may give valuable information about the DP that can be used for optimisation of the densification process, without the need of advanced technology such as X-ray densitometry.

The purpose of this study was to establish a method that can predict the DP of surface-densified wood by continuous measurement of the indentation in a hardness measurement test, in order to be able to better assess the performance of the densified surface.

2 Materials and methods

In Part 1 of the present study, defect-free Scots pine (*Pinus sylvestris* L.) specimens 50 × 21/18.5 × 50 mm (tangential × radial × longitudinal) in

***Corresponding author: Alexander Scharf**, Wood Science and Engineering, Luleå University of Technology, Forskargatan 1, SE-93187 Skellefteå, Sweden, E-mail: alexander.scharf@ltu.se
Benedikt Neyses and Dick Sandberg, Wood Science and Engineering, Luleå University of Technology, Forskargatan 1, SE-93187 Skellefteå, Sweden. https://orcid.org/0000-0002-1489-0839 (B. Neyses)

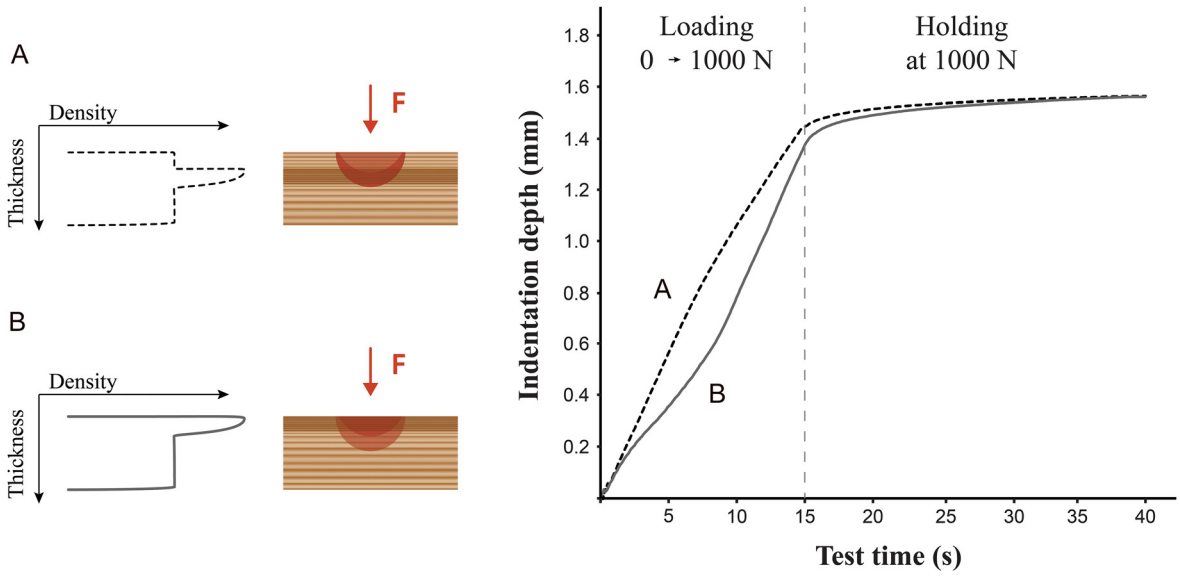

Figure 1: The development of the indentation depth in two surface-densified specimens (different process conditions) during a Brinell hardness test according to EN 1534 (CEN 2020).
Case (A) represents a specimen with a densified peak region fairly deep beneath the densified surface, and case (B) represents a specimen with a densified peak region immediately beneath its surface.

size were surface-densified in the radial direction to a thickness of 17 mm, with varied compression ratio, pressing temperature and pressing speed in the process, and the DPs in the densification direction were acquired with an X-ray DP analyser. The densified specimens were subjected to seven different hardness test methods. This paper (Part 2) covers the analysis of the indentation-versus-time curves from the hardness tests and the partial least squares (PLS) regression to predict the DP of surface-densified wood. The experimental procedure of the study (Figure 2) was performed in the following way:

(1) Preparation of the surface before densification to affect the DP
(2) Surface densification with different process parameters to create a set of specimens with large variation in the DPs and indentation-versus-time curves
(3) X-ray densitometry to measure the DP
(4) Hardness tests to measure the indentation-versus-time
(5) PLS regression to determine the relation between the indentation-versus-time curves of the hardness tests and the DPs which enables the prediction of the DP of surface-densified wood.

The experimental procedure in Part 1 gave rise to the DPs shown in Figure 3 which were used in the PLS regression. The "densified surface" is defined as the surface in contact with the heated platen during densification. There is an inherent measurement error associated with the first few measurement points in X-ray densitometry (within ca. 0.3 mm from the densified surface), where the X-ray beam covers partly air and partly wood, resulting in an underestimated density value for approx. the first seven measurement steps. This may affect the PLS regression.

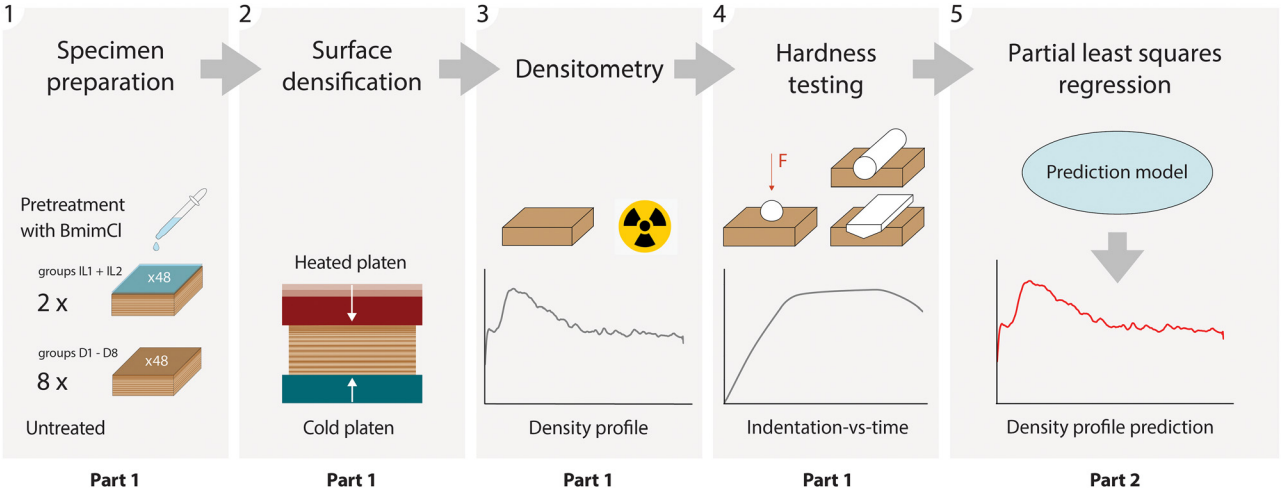

Figure 2: Experimental procedure. The multivariate data analysis (5) was carried out separately for each hardness test.

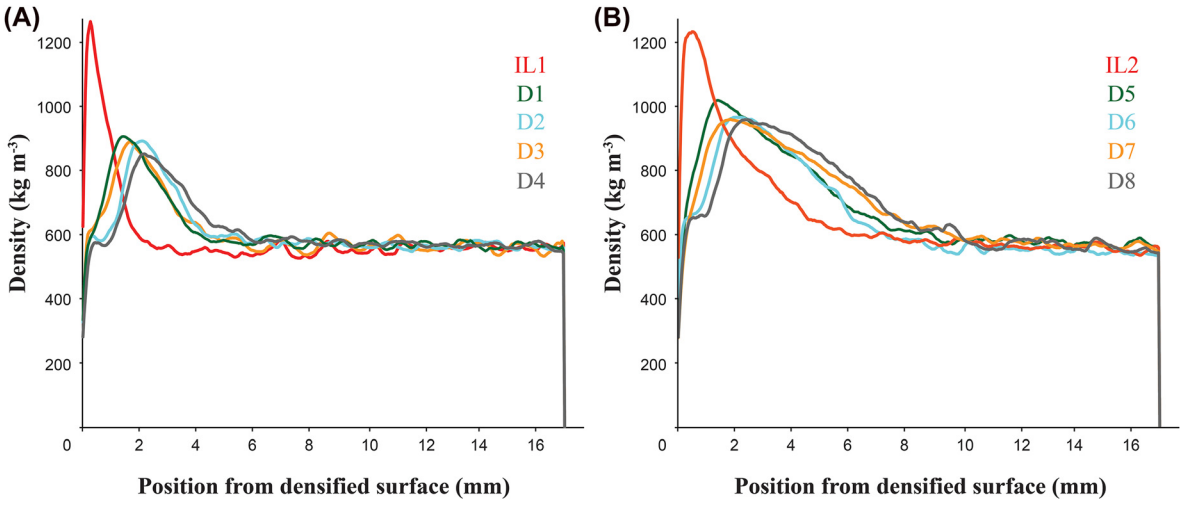

Figure 3: Average DPs of the different groups (D1–D8, IL1 and IL2, $n = 48$) of surface-densified wood with a compression ratio of (A) 8% and (B) 19%.

2.1 Analysis of hardness data

The hardness measurement curves acquired by the seven different hardness test methods were analysed prior to the multivariate modelling. For six test regimens, three different indenter geometries (sphere, cylinder and wedge) and two levels of target load (full-force and half-force) were used with force-controlled loading according to EN 1534 standard (CEN 2020). The test method names comprise these test parameters. One hardness test (Brinell-Japan) was the depth-controlled loading to 4 mm depth with a spherical indenter according to JIS Z 2101 (JSA 2009). The detailed specifications of each test and the used equipment are presented in Part 1.

The applied force and indentation depth measured by the cross-head displacement were recorded every 0.1 s in all tests, providing curves of the indentation-versus-time in the depth-controlled tests and force-versus-indentation in the force-controlled test.

2.2 Multivariate modelling and analysis

To study the relationship between the indentation-versus-time curve and the DP of the surface-densified wood, the results from each hardness test were subjected separately to a partial least squares (PLS) analysis. The SIMCA 15 (Sartorius AG, Göttingen, Germany) software was used to apply the PLS regression. PLS regression is a supervised learning algorithm that makes it possible to predict a dependent output (y-variables in PLS analysis) from a known input (x-variables) (Eriksson 2006). The variables were in this case defined as follows:

- x-variables: 550 measurements of the indentation depth at intervals of 0.1 s, each x-variable representing one time step (cf. Figure 5). In the case of the depth-controlled Brinell-Japan test, 400 x-variables describing the applied force at intervals of 0.01 mm indentation depth.
- y-variables: 385 density measurements, one for each measurement step in the densitometry, together forming the DP (cf. Figure 3).

For each specimen (observations in PLS-analysis) one value was measured for each x- and y-variable which together built up the data sets (X-matrix and Y-matrix) used in the PLS analyses (Table 1). For example, the first x-variable in the Sphere-1000N method is the vector (320×1 in size) including all measured values of indentation depth at 0.1 s test time from all 320 specimens.

The principle of the PLS analysis and prediction used in this study is shown in Figure 4. All the data were first subjected to unit variance scaling and mean-centering to normalize the dataset, which means that variables with generally small measurement values are weighted similarly to variables with large measurement values in the PLS analysis. The number of significant PLS components was determined by seven rounds of cross validation.

To evaluate the PLS models created, the hardness test method with the highest predictive ability according to the PLS model was further analysed and used to predict the DPs of an external test set, all the observations for the test method being randomly distributed into a training data set and a test data set. The PLS-model was then generated purely from the training dataset, consisting of 80% of the observations. To evaluate the model performance, the mean absolute percentage error for all the y-variables was determined from the difference between the predicted densities and both the true and averaged densities in the test dataset, consisting of the remaining 20% of the observations. A moving average with a length of 20 x-variables was used to calculate the average DP.

3 Results and discussion

3.1 Indentation-versus-time curves

The x-variables for the PLS-model consists of the measured indentation-versus-time data from the hardness tests. The average indentation-versus-time curves of three treatment groups are shown in Figure 5. The IL1 and IL2 groups exhibit the most heterogeneous DP shape and are interesting to analyse individually, while the group D4 group is representative of all D1–D8 groups without chemical pretreatment with ionic liquids (IL).

Table 1: Description of the number of *x*- and *y*-variables in the different test methods and the resulting data set size.

Test method	No. of observations (specimens)	No. of *x*-variables (indentation depth)	No. of *y*-variables (density)	*X*-matrix size (observations × *x*-variables)	*Y*-matrix size (observations × *y*-variables)
Sphere-1000N	320	550	385	(320 × 550)	(320 × 385)
Sphere-500N	320	550	385	(320 × 550)	(320 × 385)
Brinell-Japan	320	400	385	(320 × 400)	(320 × 385)
Cylinder-2500N	160	550	385	(160 × 550)	(160 × 385)
Cylinder-1250N	160	550	385	(160 × 550)	(160 × 385)
Wedge-2500N	160	550	385	(160 × 550)	(160 × 385)
Wedge-1250N	160	550	385	(160 × 550)	(160 × 385)

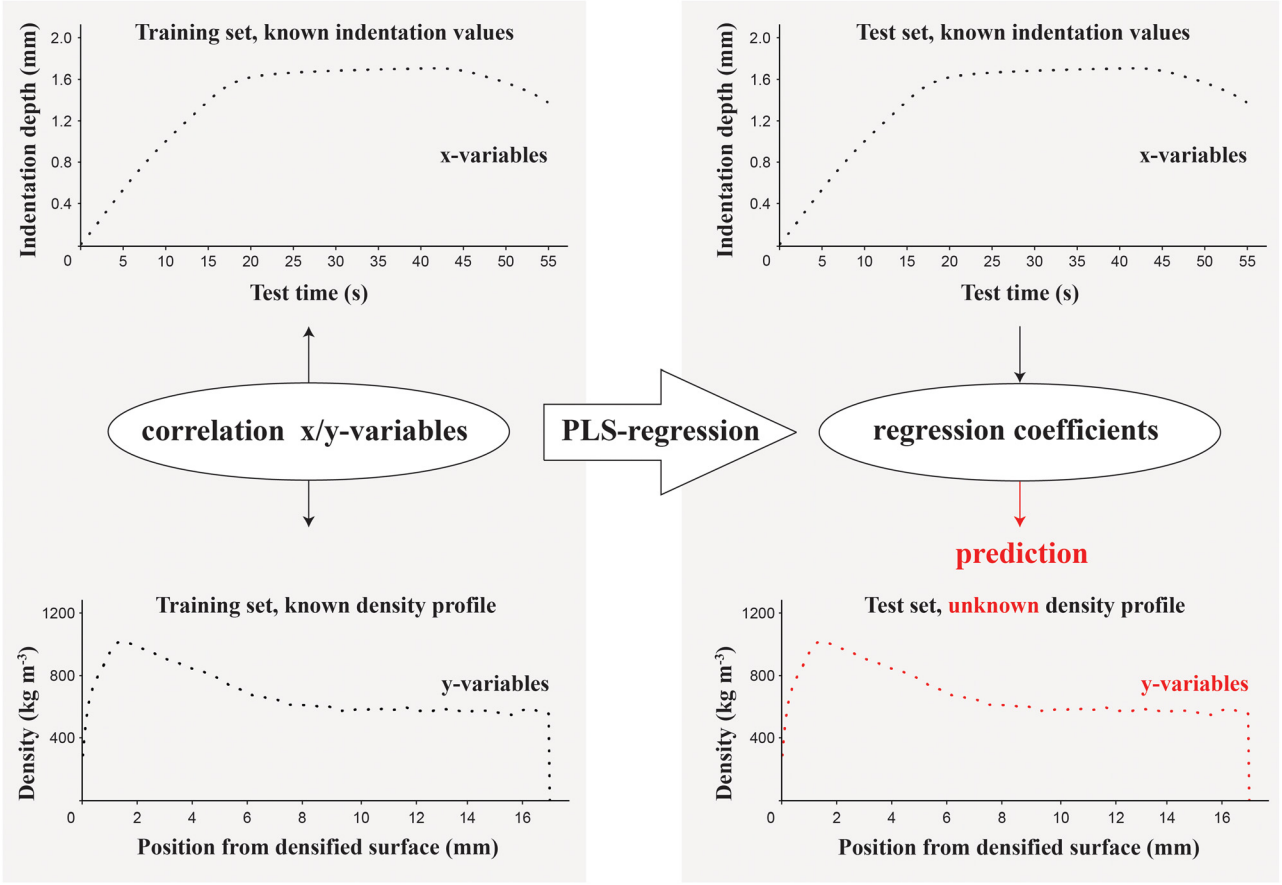

Figure 4: The principle of PLS analysis applied in this study. The relations between the measured indentation depths (*X*-matrix) and the DPs (*Y*-matrix) in the training dataset are determined by PLS-regression analysis. The output, in the form of regression coefficients, is used in combination with the indentation-versus-time data of new observations (test set) to predict the unknown DPs. Each data point on the *x*-axis represents an individual *x*/*y*-variable.

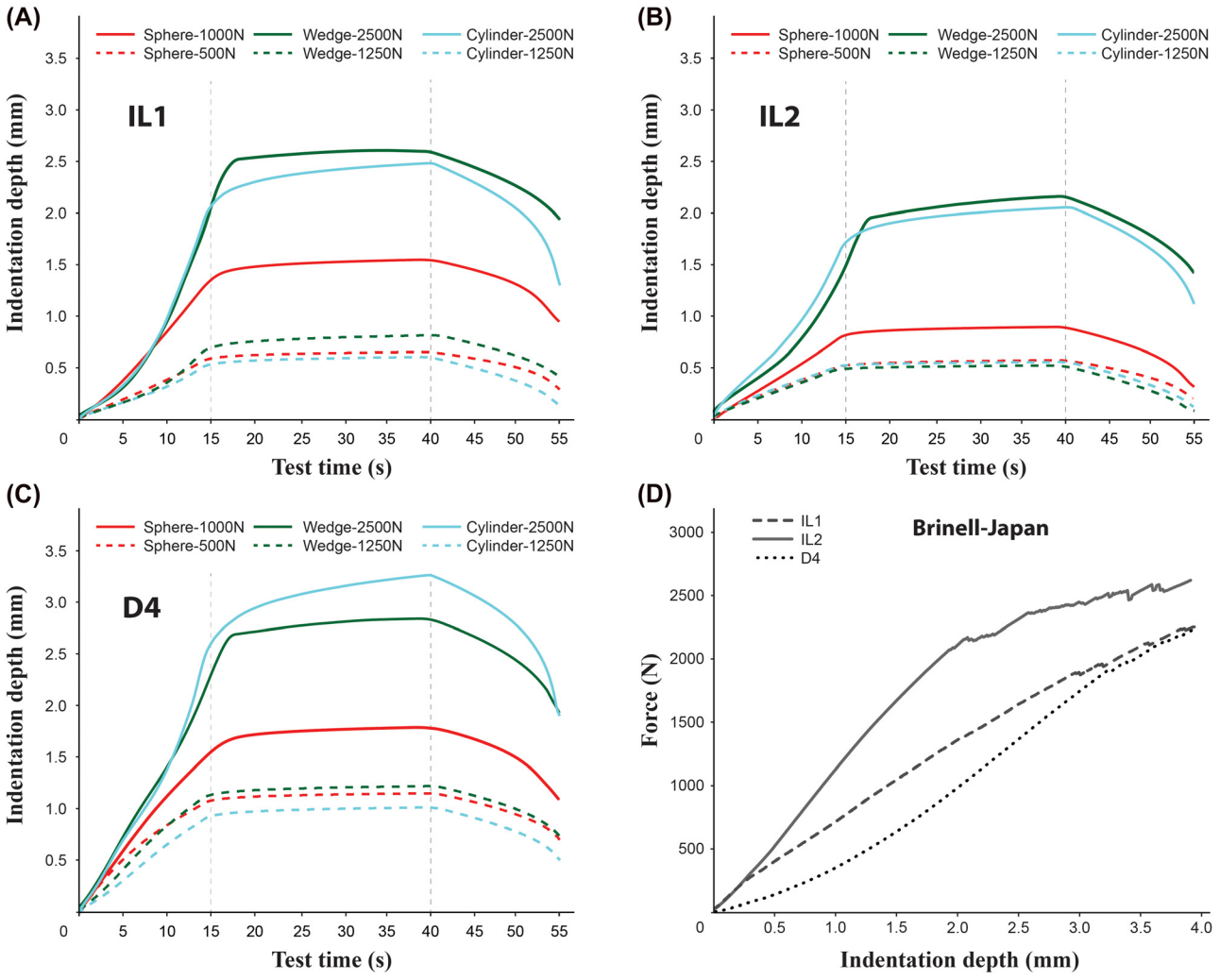

Figure 5: Average indentation-versus-time curves obtained by different test methods for three sample groups. (A) IL1, (B) IL2, and (C) D4. The vertical dashed lines indicate the different sections of the loading regime which are loading (0–15 s), holding the load (15–40 s), and release of the load (40–55 s). The force-versus-indentation measured with the Brinell-Japan test method is shown in (D). The load cell of the hardness testing machine was limited to a test force of 2500N and the Brinell-Japan tests stopped when this force was reached.

The curves shown in Figure 5 depend on the test method, the applied force and the sample treatment group (IL1, IL2, D4), where a high indentation depth indicates a low resistance and a low indentation depth indicates a high resistance to the indenter in Figure 5A–C. The slope of the curve indicates the amount of wood compression caused by the indentation force during a given interval of a hardness test. Since resistance to compression is known to be related to density, a steep slope indicates a higher degree of wood compression and hence a lower density than a shallow curve where less compression occurs due to the higher density of the stressed wood volume. Over the course of a complete hardness test an increasing volume of wood is stressed by the applied force and the slope of the indentation-versus-time curve changes depending on the change in test force and on the change in density and volume of the stressed wood. The changes in the slope during different time intervals (Figure 5A–C) or during different indentation depth intervals (Figure 5D) can thus describe the density distribution in the direction of indentation, i.e. the DP.

An increase in the slope during the loading phase (0–15 s) of the force-controlled tests indicates that the stress induced by the applied force is reaching the undensified region further in the core of the specimens. This is observed in the groups with the densified core close to the surface (IL1 and IL2). The opposite can be observed in the D4 group, where the region directly beneath the surface is not densified. The Wedge-2500N and Cylinder-2500N test methods show the greatest average indentation depths and the most rapid changes in slope during the loading phase.

The densified layers in the IL1 and IL2 groups were only 1–1.5 mm thick and the stresses reached the undensified core early in the test procedure. With a lower test force, this does not happen so often, resulting in low indentation depths in the half-force tests (dashed lines). There was little difference in indentation depth between the half-force tests in Figure 5. The indentation depths reached were relatively low and the indenter geometry had less influence at these depths.

The second phase of the test procedure (15–40 s) shows the amount of creep occurring in the specimens, while the load was held constant. Creep was most evident in the Cylinder-2500N test method and can be attributed to the high forces and the resulting sinking-in of the specimens.

The third phase of the test procedure (40–55 s) shows the behaviour of the specimens when the applied force was gradually lowered to zero over a period of 15 s. The elastic recovery was highest when the applied force led to a stress mainly in the densified regions. The elastic recovery was largest in the half-force tests on the IL-treated groups, where the stresses were limited to regions close to the surface. With increasing hardness test-induced compression of undensified regions the elastic recovery decreased as shown in Figure 5C in the Cylinder-2500N and Wedge-2500N tests.

Figure 5D shows the Brinell-Japan test, i.e. the force required to press the spherical indenter to a given depth for the three representative test groups. The slope of the individual curves provides a good picture of the density distribution, where the forces required for indentation into the IL-treated specimens were similar to each other in the beginning of the test but where, with further indentation depth, the thinner densified region in the IL1 group (compression ratio 8%) was overcome and the slope angle decreased, which was not the case in the IL2 group (compression ratio 19%). The D4 group behaved differently because the densified region is located further beneath the specimen surface.

3.2 Partial least squares analysis

The DPs and indentation-versus-time curves exhibit a relationship which can be determined by partial least squares analysis. The predictive ability or correlation was the main model evaluation criterion used in this study. The metric Q^2 is the coefficient of determination between the indentation-versus-time curves and DPs and describes the total proportion of variation within the *Y*-matrix that can be predicted by the cross validation. The total predictive ability (Q^2cum) and the predictive ability for individual *y*-variables (Q^2V) were considered in the model evaluation. Q^2cum describes the average Q^2V-values of all *y*-variables and is a useful indicator for the overall model performance. A Q^2V-value of 1 for a specific *y*-variable is equivalent to a 100% accurate prediction of the values of a *y*-variable and means that the density at that depth beneath the densified surface is well explained by the model, because the variation in that *y*-variable at that depth in the dataset is highly correlated to the variation in the indentation-versus-time curves (*X*-matrix). For PLS-modelling of bio-based materials, a Q^2V-value greater than 0.5 can be considered to show good predictive ability (Eriksson 2006). A Q^2V-value for a *y*-variable of 0.5 means that 50% of the variation in that *y*-variable can be explained by the variation in the indentation-versus-time curves. The remaining 50% of the variation is caused by material and testing parameters which are not included in the dataset for the PLS-modelling.

Figure 6 shows the Q^2V-value for each *y*-variable for all seven hardness tests, all the *y*-variables being predicted independently of each other.

The Q^2V-values of *y*-variables close to the densified surface are high (ca 0.8) for all seven hardness tests methods. The Q^2V-value decreases with increasing distance from the densified surface indicating that there is less interaction between indenter and wood far from the test surface. If the Q^2V-value is close to 0 the wood beneath the densified surface is not affected at all by the intender and the DP cannot be predicted. Since the correlation between density far from the densified surface and hardness is low it is not of interest for assessing the performance of surface-densified wood. A Q^2V-value greater than 0.5 within the compressed zone, i.e. 0–10 mm beneath the densified surface (cf. Figure 3), was achieved only with the methods Brinell-Japan, Sphere-1000N and Wedge-2500N.

The increase in the resolution of the indentation depth measurement in the test by using only 50% force (dashed line in Figure 6) did not lead to a higher correlation, and the use of 50% target force thus does not provide a more detailed model for the prediction of density close to the surface.

In Figure 6 the Q^2V-values are low in the 0–0.3 mm zone beneath the densified surface. The measurements at the beginning of the hardness tests are characterised by a high variation, presumably due to the slightly uneven specimen surfaces, which settle and become distorted when they are stressed during the initial load application. The elongated geometries of the wedge and cylinder tend to lead to uneven contact in the initial contact phase, increasing this variation. In the Sphere-1000N test method, however, the spherical geometry of the indenter gave a tight contact between the wood and the indenter from the beginning of the test, and the high force led to a more rapid settlement of uneven samples, which is presumably the

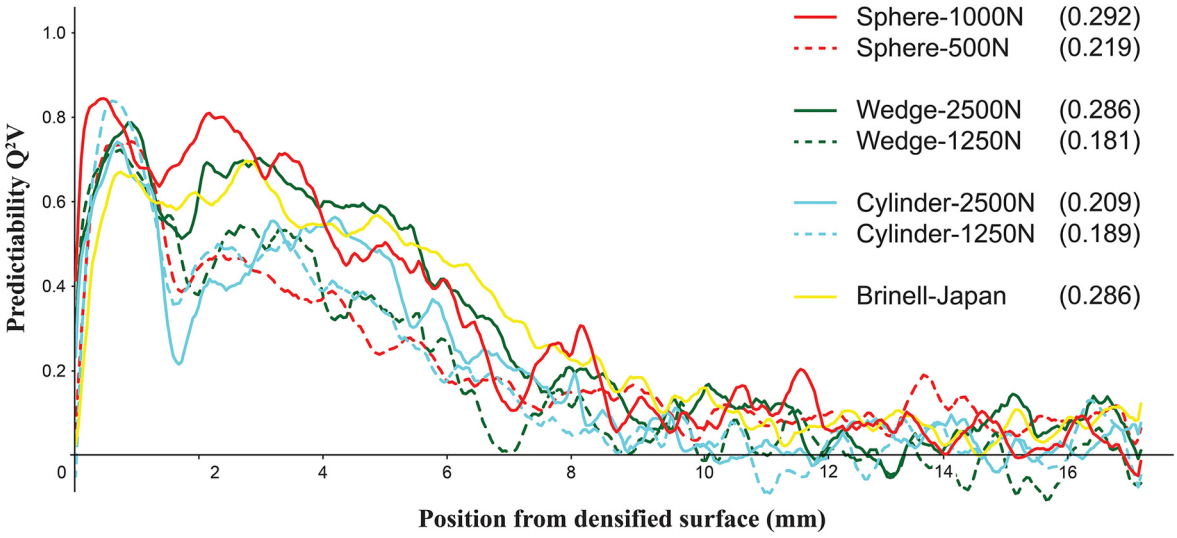

Figure 6: Predictive ability for each *y*-variable (Q^2V) for all tested indentation methods. Q^2cum for each model is shown in the legend.

reason why this method has the highest Q^2V close to the densified surface.

The similarity between the locations of the density peaks in Figure 3, and the position of the peak-values of Q^2V, suggests that these positions of highest prediction are congruent with the positions of the density peaks in the true DPs and that the position of the density peak has a strong influence on the indentation-versus-time curve (cf. Figure 5). The D1–D8 groups exhibit density peaks at 2–2.5 mm from the surface and the IL1 and IL2 groups within 0.5 mm from the surface. The densification process parameters did not result in specimens with their density peak between these regions to increase the dataset variation. Between the two peak regions, a distinct drop in the Q^2V-values was observed. In general, a higher variation within the training dataset leads to a higher performance of the prediction model (Therrien and Doyle 2018).

For each *y*-variable a regression coefficient is obtained for each *x*-variable. The *x*-variables can be grouped into the loading, load holding and unloading phases of the hardness test methods and analysed individually. The correlations in the loading phase and holding phase are in line with the results of the overall correlation (cf. Figure 6), but the correlation in the holding phase did not change after 10 s of holding time (except when sinking-in was occurring). The correlation during the unloading phase was close to zero, indicating that the elastic recovery of the material was not related to the DP of the material, and that a test method could be limited to 15 s of loading and 10 s of holding time without weakening its predictive ability.

The Sphere-1000N test shows the highest Q^2cum and thus provides the most accurate prediction of the DP. The Q^2V-values of the PLS-model show the relationship between the variables, but to fully evaluate the performance of the PLS-model, the DPs of observations which had not been included in the building of the model had to be evaluated. The DPs of an external test set predicted by the Sphere-1000N hardness test are shown in Figure 7. Similar results were achieved by the PLS-analyses of hardness test methods having a similar Q^2cum, such as Wedge-2500N and Brinell-Japan.

The overall shape of the DPs and the peak density values are predicted well by the PLS-model, Figure 7A shows that the growth-ring density variation in the DP is not predicted by the PLS-model. In the PLS-analysis, a smooth DP curve without density variations (Figure 8A) such as growth-ring variations is preferable for a high correlation between the *X*-matrix and the *y*-variables. A growth-ring orientation almost parallel to the X-ray gives a characteristic wavy density pattern, as shown in Figure 8B from a depth of 6 mm. This variation in density measured does not affect the indentation-versus-time curve and this means that the prediction by the model is less accurate, particularly in undensified areas located at large distances from the densified surface or close to the surface in specimens compressed at higher temperatures, e.g. up to 1 mm from the surface in Figure 8A.

The width of the growth rings is probably too narrow to influence the indentation-versus-time curve in the hardness tests. By comparing the predicted density values to an average value of the observed density values, the influence of the growth-ring density variations can be reduced. A prediction of the general DP shape, without growth-rings, can be valuable in a process control situation since the

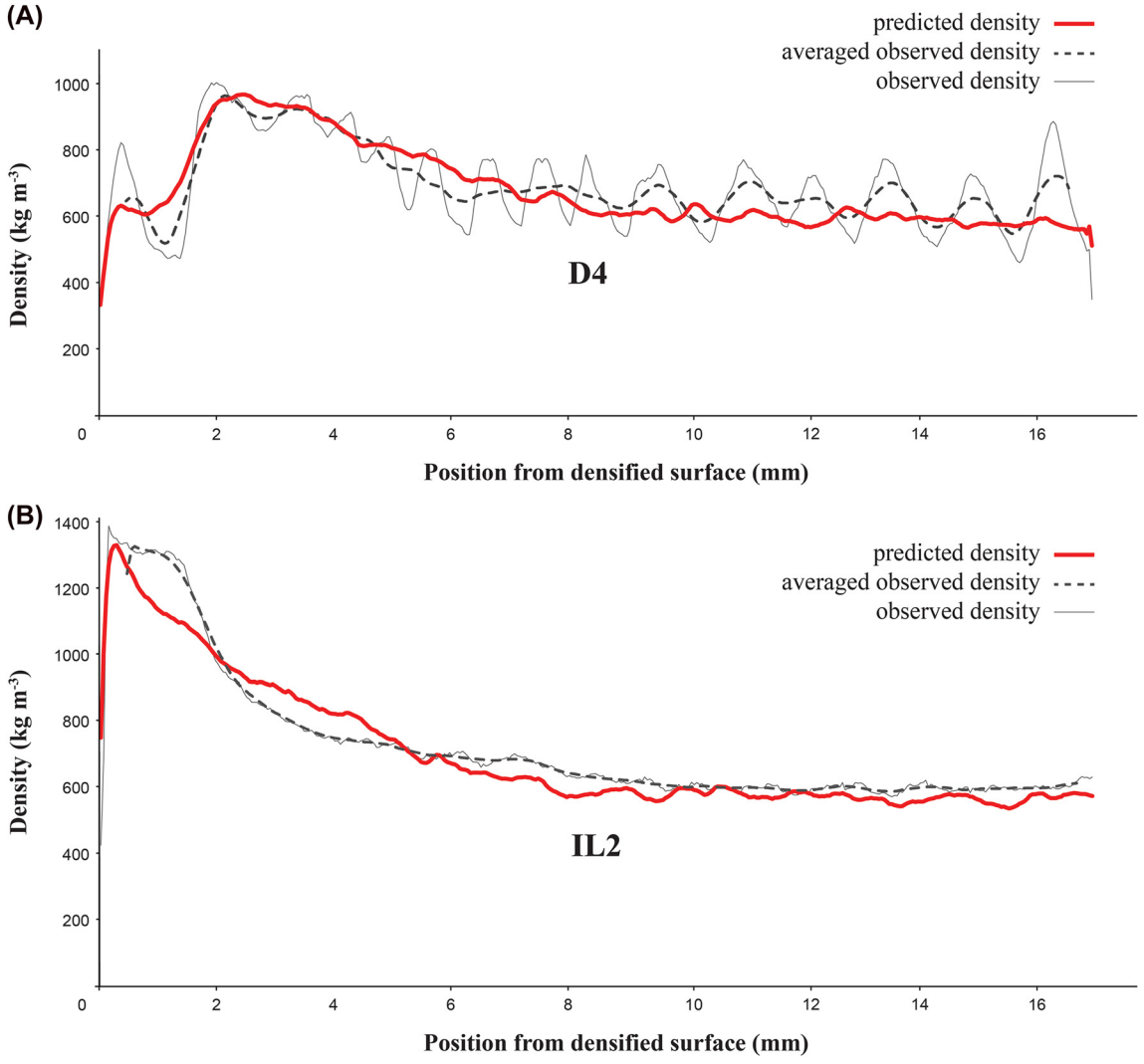

Figure 7: Examples of observed and predicted DPs of specimens in the test set. Each DP represents a single specimen. (A) a specimen with distinct growth rings in the DP and densified without chemical pre-treatment from the D4 group, and (B) a specimen without distinct growth rings in the DP and densified after pre-treatment with IL from the IL2 group.

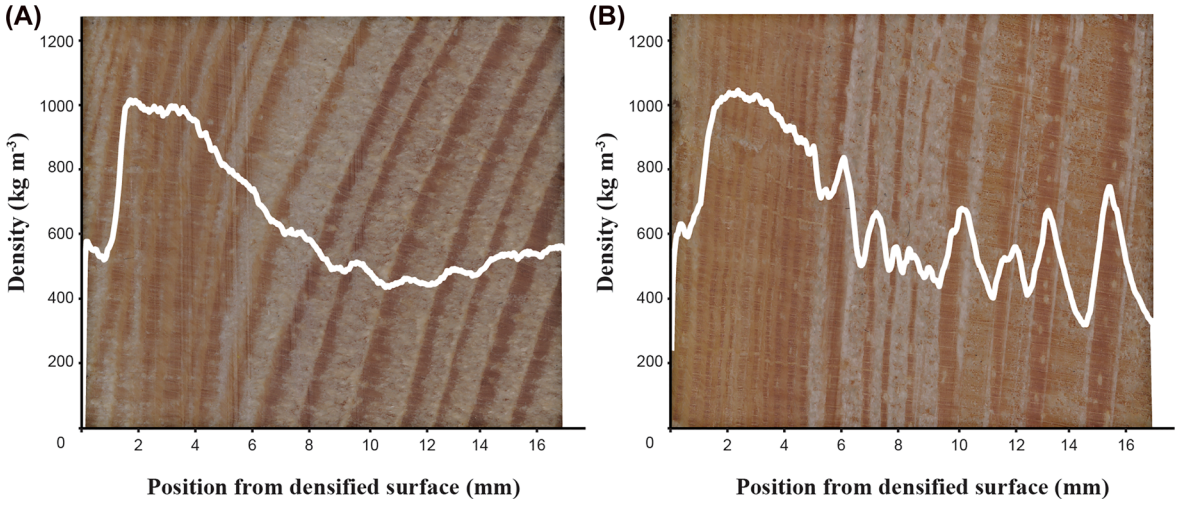

Figure 8: The influence of the growth-ring orientation on the DP measured with a X-ray orientation parallel to the densified surface. The step-wise measurement of density leads to either (A) indistinct or (B) distinct growth-rings pattern in the DP. A small deviation in growth-ring orientation may influence the shape of the DP to a great extent.

hardness of the final material may be independent of the growth-ring angle.

Figure 7B shows a specimen with a strong and wide peak caused by densification and pre-treatment with IL. The peak density is predicted but not the exact shape. Stress fields occur below the indenter and expand with increasing load, and the resistance of the material to the indentation is thus determined by the behaviour of the whole stressed volume. It is possible that different peak shapes in the DPs may lead to similar indentation-versus-time curves, and this may limit the prediction performance.

A general evaluation of the ability of the Sphere-1000N PLS-model to predict the DP for the whole test set is shown in Figure 9, where the mean absolute percentage error between the observed and predicted density values is plotted as a function of position from the surface. The test set consisted of a total of 64 observations from all 10 specimen groups.

On average the predicted values deviate by between 5 and 10% from the observed values. The prediction error for the observed (dashed line) and the averaged observed density values (continuous line) differ depending on the position in the sample. The true and average density values are close to each other in densified regions because of the compression and the disappearance of growth-rings in the DPs in these regions.

The prediction error is very high for the first 0.5 mm because of measurement inaccuracies in the hardness test and densitometry. It was, however observed that the prediction error of values of *y*-variables close to the surface was higher for IL-treated specimens than for the traditionally densified specimens (not shown). This narrow layer of high density appears to have a minor effect on the indentation-versus-time curve so that it cannot be predicted accurately. The brittle failure of the wood surface observed mainly in the IL1 group supports the suggestion that surface densification must create a sufficiently wide densified area in order to increase the effective resistance of the material to a point load.

The error is lowest for *y*-variables at a distance of about 2 mm from the densified surface, where most of the density peaks of the specimens were located. The prediction error did not increase between 9 and 17 mm (Q^2V-value ~ 0, cf. Figure 6), because there was little variation in density in the training and tests set in the undensified area.

The prediction model could be improved by reducing the amount of noise in both the *X*-matrices and *Y*-matrices, by excluding observations or re-measuring DPs with strong

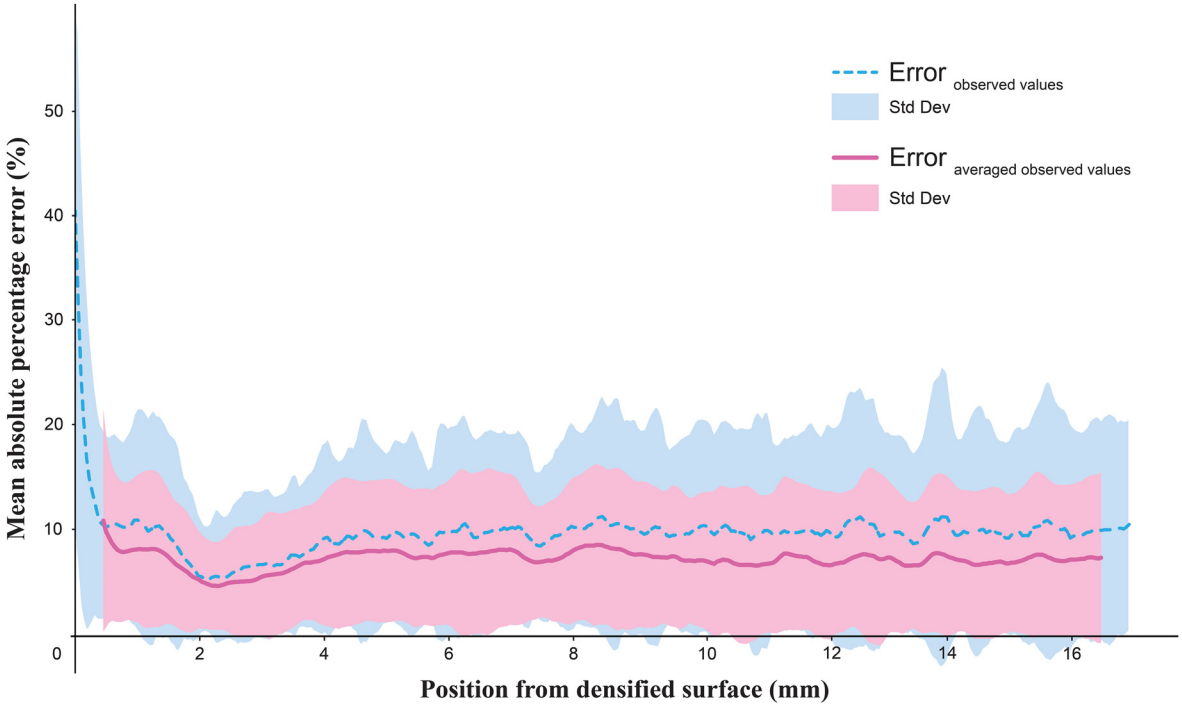

Figure 9: Mean absolute percentage error for the prediction of the DP of the external test set by measuring hardness according to Sphere-1000N. The filled areas express one standard deviation of the absolute percentage error. The continuous line and the red area show the prediction of averaged DP-variables. The dashed line and the blue area show the prediction of the unmodified DP-variables. Each point on the *x*-axis represents a single DP-variable.

growth-ring density variations. Another way of improving the model would be to add more *x*-variables. The indentation-versus-time curve can be expressed by different derivatives of the indention depth. This would make it possible to take into consideration interaction effects between the *x*-variables, which would potentially result in a better prediction performance.

4 Conclusions

To improve the way in which the hardness of surface-densified wood is evaluated, a method has been developed to predict high-resolution density profiles of surface-densified wood solely on the basis of the indentation-versus-time curves obtained from hardness testing.

Partial least squares regression analysis, a supervised learning algorithm was applied to the indentation-versus-time curves obtained by seven different hardness testing methods, based on different forces and different indenter geometries. Density profiles obtained by X-ray densitometry were used to train the algorithm. The indentation-versus-time curves given by the Brinell method Sphere-1000N showed the highest correlation to the density profiles, and this regression model gave the best predictions of the density profiles, achieving mean absolute percentage errors of 5–10%. The hardness tests using a cylindrical indenter had the worst predictive ability. For the Sphere-1000N method, the PLS model performed well in predicting the density profile to a depth of 9 mm beneath the specimen surface. The correlation in the case of density deeper than 9 mm was zero, indicating that this region was too far from the surface of the specimen to be affected by the applied force.

The proposed method has the potential to be used in process control and process design for the optimisation of surface-densified wood products or when densitometry is not a viable option. A training data set with a more balanced distribution of DP shapes would result in a model applicable for a broader variety of DPs. Future work will include the optimisation of the prediction model and application of this approach to abrasion tests. It is possible that the hardness curve as well as the predicted DP can be used to estimate other density-related strength properties.

Author contributions: All the authors have accepted responsibility for the entire content of this submitted manuscript and approved submission.
Research funding: Financial support through CT WOOD – a centre of excellence at Luleå University of Technology supported by the Swedish wood industry – is gratefully acknowledged.
Conflict of interest statement: The authors declare no conflicts of interest regarding this article.

References

EN 1534. (2020). *Wood flooring and parquet – determination of resistance to indentation – test method*. CEN – European Committee for Standardization, Brussels.

Eriksson, L. (2006). *Multi- and megavariate data analysis*, 2nd, rev. and enlarged ed. Umeå: Umetrics AB.

Hänsel, A., Niemz, P., and Brade, F. (1988). Untersuchungen zur Bildung eines Modells für das Rohdichteprofil im Querschnitt dreischichtiger Spanplatten. Holz als Roh- Werkst. 46: 125–132.

JIS Z 2101. (2009). *Methods for the test for wood*. Japanese Industrial Standard, Japanese Standards Association: Tokyo, Japan.

Laine, K., Antikainen, T., Rautkari, L., and Hughes, M. (2013). Analysing density profile characteristics of surface densified solid wood using computational approach. Int. Wood Prod. J. 4: 144–149.

Neyses, B., Rautkari, L., Yamamoto, A., and Sandberg, D. (2017). Pre-treatment with sodium silicate, sodium hydroxide, ionic liquids or methacrylate resin to reduce the set-recovery and increase the hardness of surface-densified scots pine. iForest 10: 857–864.

Rautkari, L., Kamke, F.A., and Hughes, M. (2011). Density profile relation to hardness of viscoelastic thermal compressed (VTC) wood composite. Wood Sci. Technol. 45: 693–705.

Scharf, A., Neyses, B., and Sandberg, D. (2022). Hardness of surface-densified wood. Part 1: material or product property? Holzforschung 76, https://doi.org/10.1515/hf-2021-0151.

Therrien, R. and Doyle, S. (2018). Role of training data variability on classifier performance and generalizability. *Medical imaging 2018. Digital pathology*. International Society for Optics and Photonics: Houston, TX, USA, vol. 10581, p. 1058109.